Immunity, Vol. 10, 9–19, January, 1999, Copyright ©1999 by Cell Press

Prolonged Eosinophil Accumulation in Allergic Lung Interstitium of ICAM-2-Deficient Mice Results in Extended Hyperresponsiveness

Nicole Gerwin,[1,3,7] Jose-Angel Gonzalo,[2,3] Clare Lloyd,[2,3] Anthony J. Coyle,[2] Yvonne Reiss,[4] Naheed Banu,[5] Baoping Wang,[6] Hong Xu,[3] Hava Avraham,[5] Britta Engelhardt,[4] Timothy A. Springer,[3] and Jose C. Gutierrez-Ramos[2,3,7]

[1] Millennium Biotherapeutics
[2] Millennium Pharmaceuticals
Cambridge, Massachusetts 02139
[3] The Center for Blood Research
Harvard Medical School
Boston, Massachusetts 02115
[4] Max-Planck-Institut für physiologische und klinische Forschung
61231 Bad Nauheim
Germany
[5] Division of Hematology/Oncology
New England Deaconess Hospital
Harvard Medical School
Boston, Massachusetts 02215
[6] Division of Immunology
Beth Israel Hospital
Boston, Massachusetts 02215

Summary

ICAM-2-deficient mice exhibit prolonged accumulation of eosinophils in lung interstitium concomitant with a delayed increase in eosinophil numbers in the airway lumen during the development of allergic lung inflammation. The ICAM-2-dependent increased and prolonged accumulation of eosinophils in lung interstitium results in prolonged, heightened airway hyperresponsiveness. These findings reveal an essential role for ICAM-2 in the development of the inflammatory and respiratory components of allergic lung disease. This phenotype is caused by the lack of ICAM-2 expression on non-hematopoietic cells. ICAM-2 deficiency on endothelial cells causes reduced eosinophil transmigration in vitro. ICAM-2 is not essential for lymphocyte homing or the development of leukocytes, with the exception of megakaryocyte progenitors, which are significantly reduced.

Introduction

Leukocyte migration from the blood into surrounding tissue is critically regulated by the interplay of several families of adhesion receptors (Butcher, 1991; Lasky, 1992; Springer, 1994). Essential to this adhesion cascade is the interaction between immunoglobulin (Ig) cell adhesion receptors expressed on endothelium and integrins on leukocytes. The Ig superfamily members intercellular adhesion molecules (ICAM)-1 and ICAM-2 are products of distinct and homologous genes and were initially identified by their ability to bind the β2 integrin LFA-1 (CD11a/CD18) (Springer, 1990; de Fougerolles and Springer, 1992).

The overlapping yet distinct expression patterns of ICAM-1 and ICAM-2 in human tissue suggest specialized roles for both molecules: ICAM-2 is constitutively expressed on all vascular endothelium including high endothelial venules at much higher levels than ICAM-1 (de Fougerolles et al., 1991). In contrast, ICAM-1 expression is strongly inducible by inflammatory cytokines. Both ICAMs are expressed at low levels on most leukocytes including T and B lymphocytes, monocytes, macrophages, NK cells, eosinophils, and $CD34^+$ early hematopoietic progenitor cells (de Fougerolles et al., 1991; Mendelson et al., 1995; N. G. and J. C. G.-R., unpublished data). Interestingly, ICAM-2 but not ICAM-1 is expressed on megakaryocytes and on both resting and activated platelets (Diacovo et al., 1994). LFA-1, the common ligand of ICAM-1 and ICAM-2, is found on virtually all cells of myeloid and lymphoid lineages, including eosinophils, and is upregulated on the surface of activated leukocytes (Kishimoto et al., 1989; Arnaout, 1990; Resnick and Weller, 1993). In vitro, ICAM-2 accounts for about two-thirds of the LFA-1-dependent adhesion of lymphocytes and monocytes to resting endothelial cells, while ICAM-1 mediates one third of the binding (Dustin and Springer, 1988; de Fougerolles et al., 1991; Xu et al., 1994).

Based on the expression patterns of ICAM-2 and ICAM-1, it has been hypothesized that ICAM-2 is important for leukocyte trafficking in uninflamed tissues, as in lymphocyte recirculation, whereas induction of ICAM-1 on endothelium and other cells by inflammatory cytokines may increase cell-cell interactions and leukocyte extravasation at inflammatory sites (Springer, 1994). ICAM-1-deficient mice are resistant to septic shock (Xu et al., 1994) and show attenuated ischemia reperfusion injury (Connolly et al., 1996; Kelly et al., 1996; Soriano et al., 1996).

Airway hyperresponsiveness is one of the central features of asthma (Cockcroft et al., 1977). Reversible narrowing of the airways is generally observed in association with pulmonary inflammation (Gelfand and Irvin, 1997). The inflammatory infiltrate in the lung is characterized by an increase in number of eosinophils, which are central to the pathogenesis of the disease (Gleich et al., 1988). The recruitment of these cells to the site of inflammation is controlled by adhesive interactions to endothelial, epithelial, and other tissue resident cells. In mouse models of allergic airway inflammation, the recruitment of leukocyte subsets to the lung can be monitored at different anatomical sites: interstitial (perivascular and/or airway wall) and airway lumen. These anatomical locations correspond to different degrees of leukocyte migration, from essential blood vessel extravasation, navigation through tissue interstitium, to transepithelial exit to airway lumen. Even more importantly, these models also make it possible for us to study a physiological endpoint that is essential in disease: bronchial hyperresponsiveness (BHR).

The biological functions of ICAM-2 in vivo have not

[7] To whom correspondence should be addressed (e-mail: gerwin@mpi.com [N. G.], gutierrez@mpi.com [J. C. G.-R.]).

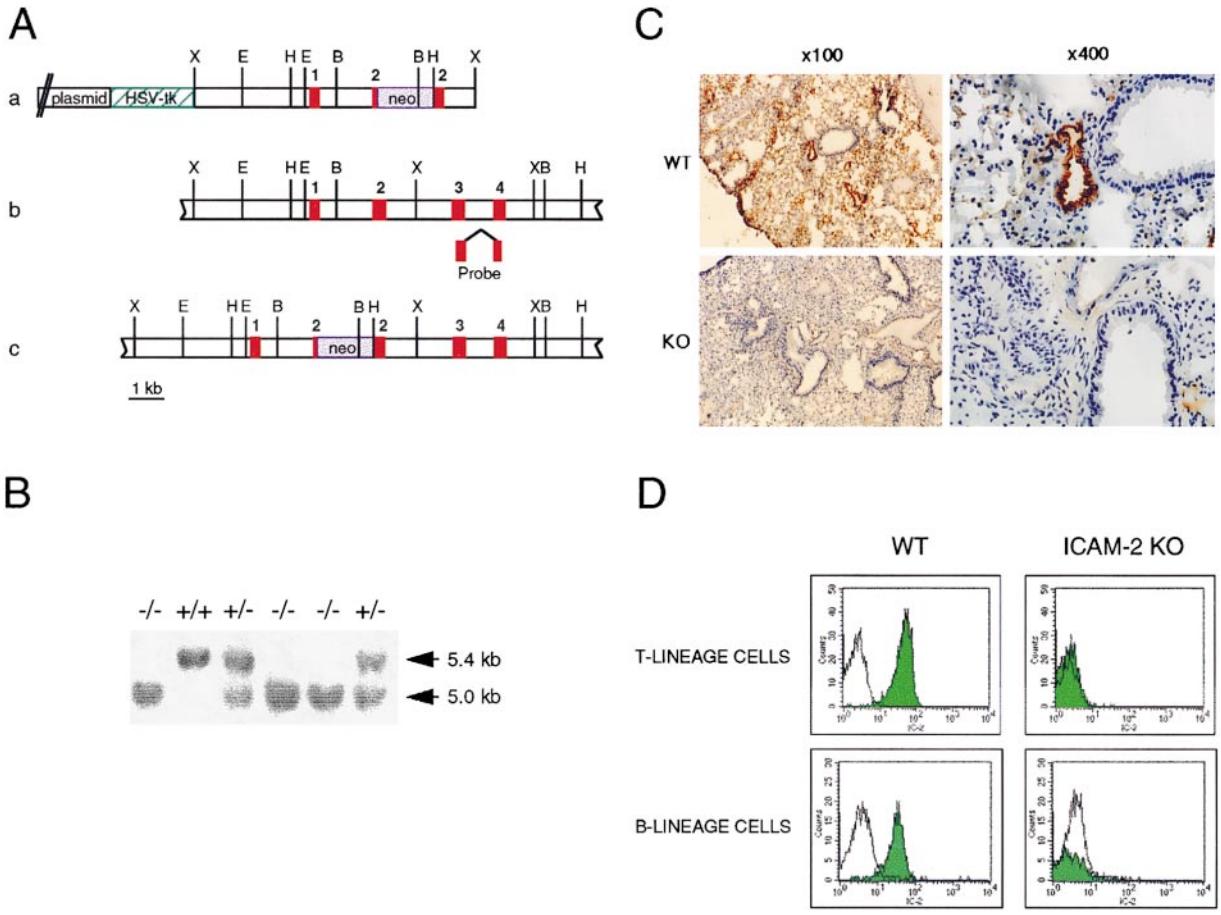

Figure 1. Targeting of the ICAM-2 Gene

(A) Design of the replacement vector. Diagrams depict the structures of the targeting vector (a), the ICAM-2 gene (b), and the mutated allele (c). The replacement vector contains the PGK-*neo*^{r} gene cassette inserted in exon 2, flanked by 5.2 and 1.1 kb of DNA from the ICAM-2 locus. The probe (a PstI/NheI cDNA fragment) is an external probe used for Southern hybridization. Restriction sites: X, XbaI; E, EcoRI; H, HindIII; B, BamHI.

(B) Southern blot analysis of tail DNA isolated from a litter of 6 mice from a heterozygous intercross. The 5.4 kb wild-type and 5.0 kb targeted allele BamHI fragments identified by the probe are indicated. The genotypes of the tested mice are shown on top of each lane.

(C) Immunohistochemical analysis of ICAM-2 expression in lung. Frozen sections of lungs from wild-type (WT; top) and ICAM-2$^{-/-}$ mice (KO; bottom) were stained with polyclonal α-ICAM-2 serum using an avidin-biotin peroxidase system in conjugation with a hematoxylin counterstain. ICAM-2 expression is visible as brown staining on vascular endothelium and alveolar capillaries (magnifications, $\times$100 and $\times$400).

(D) Flow cytometry analysis of ICAM-2 expression on lymphocytes. Thymocytes (top) and lymph node cells (bottom) from wild-type (WT) and ICAM-2$^{-/-}$ mice (ICAM-2 KO) were stained with α-ICAM-2 MAb (gray histogram) or an isotype-matched negative control MAb (white histogram) and subjected to flow cytometry.

been investigated previously. Here, we report the generation of mice that are deficient for ICAM-2 by homologous recombination in embryonic stem (ES) cells. We have used these mutant mice to study the specific role of ICAM-2 during an inflammatory response in a mouse model of allergic lung inflammation. We have also investigated the essential roles of ICAM-2 in vivo in the development of hematopoietic cells and in lymphocyte homing.

Results

Generation of ICAM-2-Deficient Mice

To generate ICAM-2-deficient mice, a gene replacement vector was made in which exon 2 (Xu et al., 1992) is interrupted by insertion of the PGK*neo* cassette (Figure 1A). J1 ES cells were transfected, selected, screened by Southern blot analysis, and microinjected into C57BL/6 blastocysts. One chimeric male transmitted the mutant allele to his offspring. Southern blot analysis of tail biopsies revealed the presence of homozygous mutant mice (ICAM-2$^{-/-}$; Figure 1B) at the expected ratios. ICAM-2$^{-/-}$ mice appeared normal in size, general health, fertility, and longevity.

Immunohistochemical staining of frozen sections of wild-type mice showed ICAM-2 positive staining in lung on vascular endothelium and alveoli but not in the large airways (Figure 1C). ICAM-2 expression in kidney, liver, and spleen resembled the expression pattern previously reported for human tissues (de Fougerolles et al., 1991; data not shown). In contrast, ICAM-2$^{-/-}$ mice were completely negative for ICAM-2 staining in these organs (Figure 1C; data not shown). Flow cytometry analysis of thymocytes, T and B lymphocytes, as well as myeloid

Table 1. Summary of Hematopoietic Development and Function Assays Performed with ICAM-2$^{-/-}$ Mice

Activity Tested	Readout	Result
NK cell cytotoxicity (n = 3)[a]	%YAC-1 lysis (±SEM); E/T ratio: 11, 33, 100, 200	WT: 10 (± 1.0), 20 (± 1.5), 24 (± 2.2), 35 (± 4.2) KO: 10 (± 1.2), 20 (± 1.1), 25 (± 3.0), 36 (± 3.0)
LAK cell cytotoxicity (n = 3)[a]	%YAC-1 lysis (±SEM); E/T ratio: 7, 22, 66, 200	WT: 5 (± 0.9), 15 (± 1.8), 32 (± 3.7), 56 (± 3.1) KO: 5 (± 0.4), 15 (± 1.0), 34 (± 2.0), 56 (± 1.8)
CFU-GM (n = 6)[b]	Number of CFU-GM per 10^6 bone marrow (BM) cells (±SEM)	WT: 2770 (± 794) KO: 2088 (± 596) p = 0.51
CFU-MK[c]	Number of CFU-MK per 2×10^5 BM cells (±SD); IL-3 conc: 0, 25, 50, 100 ng/ml	WT: 0, 8.5 (± 0.7), 9.5 (± 2.1), 13.5 (± 0.7) KO: 0, 1.5 (± 0.7), 2 (± 0), 3.5 (± 0.7)
Immature megakaryocytes[c]	Number of single megakaryocytes per 5×10^4 fract. BM cells (±SD) IL-6 conc: 0, 25, 50, 100 ng/ml mTPO conc: 0, 25, 50, 100 ng/ml	IL-6: WT: 22 (± 2.1), 49 (± 2.1), 41 (± 1.4), 34 (± 2.1) KO: 8 (± 1.4), 15 (± 1.4), 14 (± 0), 12 (± 1.4) mTPO: WT: 22 (± 2.1), 67 (± 2.1), 75 (± 0.7), 54 (± 1.5) KO: 8 (± 1.4), 12 (± 0), 18 (± 1.4), 15 (± 0.7)
Platelet count (n = 15)	Platelet number $\times 10^5/mm^3$ (±SEM)	WT: 9.5 (± 3.7) KO: 7.5 (± 3.8) p = 0.72
Bleeding times (n = 15)	Bleeding time (sec) (±SEM)	WT: 70.9 (± 12.9) KO: 63.3 (± 8.2) p = 0.63

[a] In one representative out of four experiments.
[b] Each assay was performed in duplicate.
[c] In one representative out of three experiments.

cells from a variety of organs of the mutant mice confirmed the absence of ICAM-2 expression, whereas wild-type littermates showed low but clear expression in these leukocyte types (Figure 1D; data not shown). In ICAM-2$^{-/-}$ leukocytes, ICAM-1 expression was not increased compared to wild-type hematopoietic cells (data not shown).

Effects of ICAM-2 Mutation on Hematopoietic Cell Development

In ICAM-2$^{-/-}$ mice, no significant differences were detected in the total leukocyte and red blood cell counts or leukocyte subset numbers (data not shown) compared to wild-type mice.

No significant differences between ICAM-2$^{-/-}$ and wild-type mice were detectable in the endogenous NK cell cytotoxicity in the spleen against NK sensitive YAC-1 target cells and NK resistant EL-4 target cells (Table 1; data not shown). We also observed that lymphokine-activated killer (LAK) cells in the spleen of ICAM-2$^{-/-}$ and wild-type mice kill YAC-1 and EL-4 target cells, respectively, with the same efficiency (Table 1; data not shown).

The numbers of early myeloid progenitor cells in bone marrow, spleen, and peripheral blood were determined by colony forming unit-granulocyte/macrophage (CFU-GM) assays and proved to be equal in ICAM-2$^{-/-}$ and wild-type mice (Table 1; data not shown).

Numbers of megakaryocyte progenitors at two different stages of differentiation were determined using the colony forming unit-megakaryocyte (CFU-MK) and the single cell megakaryocyte growth assay (Banu et al., 1995). In the bone marrow of ICAM-2$^{-/-}$ mice, numbers of mIL-3-dependent CFU-MK were clearly reduced, while mTPO-dependent CFU-MK were affected to a lesser extent by the lack of ICAM-2 expression (Table 1; data not shown). In the single cell assay, numbers of IL-6- and mTPO-dependent megakaryoblasts were also reduced in the ICAM-2$^{-/-}$ mice in comparison to wild-type mice (Table 1).

Platelet numbers in untreated mice or after chemotherapy-induced thrombocytopenia were unaffected by the ICAM-2 deficiency (Table 1; data not shown). In addition, bleeding times in wild-type and knockout mice were not significantly different, as shown in Table 1.

Severely Compromised Eosinophil Accumulation in Lung Allergic Inflammation in ICAM-2$^{-/-}$ Mice

To address the role of ICAM-2 in the migration of different types of leukocytes to sites of an inflammatory response, we used a mouse model of ovalbumin (OVA)-induced lung allergic inflammation in which preimmunized mice (day 1) were challenged by repeated aerosolized exposure to OVA (day 8 and days 15–21, daily). This model is characterized by macrophage, lymphocyte, and eosinophil accumulation in both the lung interstitium and the airway lumen, in conjunction with development of BHR (Gonzalo et al., 1996a, 1998).

Eosinophil numbers in the airway lumen as determined by bronchoalveolar lavage (BAL) reach their maximum 3 hr after the antigen challenge on day 21 in this mouse model (Gonzalo et al., 1996a; Figure 3A). In ICAM-2-deficient mice, BAL eosinophil numbers on day 21, 3 hr after OVA treatment, were reduced by 77.8% as compared to wild-type mice (Figure 2A). No significant reduction in BAL lymphocyte, monocyte, and macrophage numbers was detectable.

Mechanism of ICAM-2 Controlled Eosinophil Accumulation in the Airway Lumen

Eosinophil numbers in either bone marrow or peripheral blood after OVA treatment were not significantly different in ICAM-2$^{-/-}$ and wild-type mice, ruling out the possibility that ICAM-2 deficiency affects eosinophil development.

ICAM-2 does not seem to be essential for lymphocyte, monocyte, or macrophage accumulation in the airway lumen, since in ICAM-2$^{-/-}$ mice the lymphocyte, monocyte, and macrophage infiltrates were not reduced. In ICAM-2$^{-/-}$ and wild-type mice, the lymphocyte infiltrate was composed predominantly of T lymphocytes, as shown by immunostaining of BAL cells with Thy1.2 MAb (data not shown).

The levels of the Th2 cell cytokines IL-4 and IL-5, as

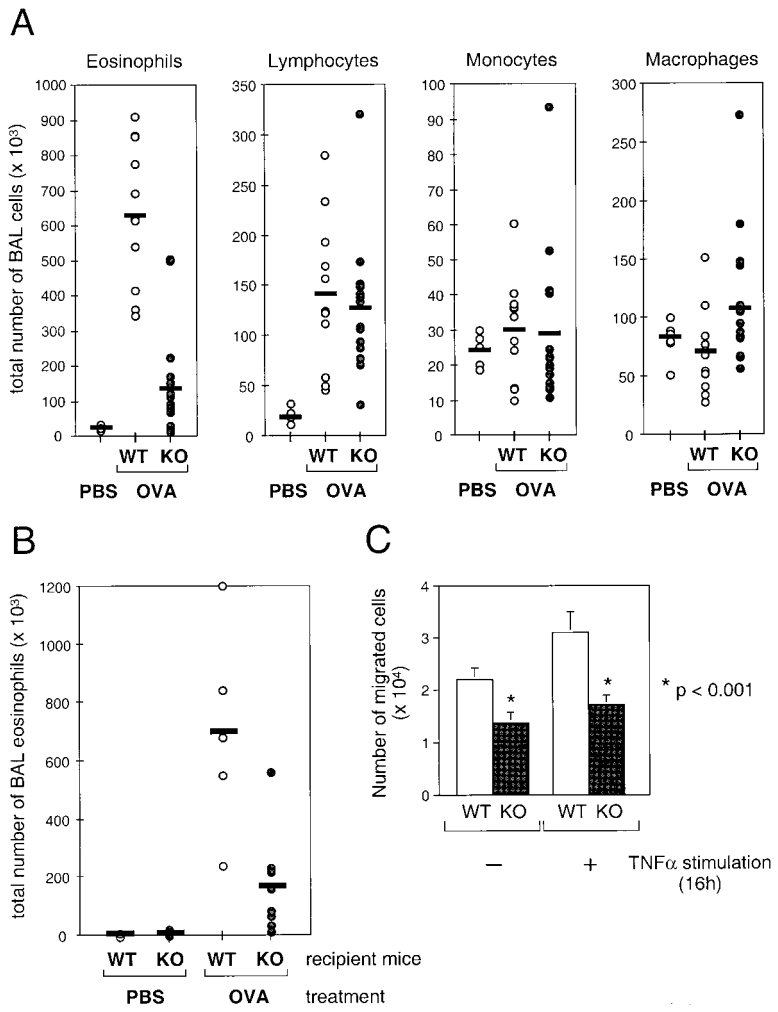

Figure 2. Reduced Eosinophil Accumulation in the Airway Lumen of ICAM-2$^{-/-}$ Mice upon OVA Treatment Is Controlled by Nonhematopoietic Cells

(A) Leukocyte numbers in the BAL 3 hr after the last OVA administration on day 21. A control group consists of wild-type mice that were treated with PBS instead of OVA. Each circle represents a single wild-type (WT; open circle; n = 11) or ICAM-2$^{-/-}$ (KO; closed circle; n = 14) mouse. Bars represent the mean of each group. The reduction in the average number of eosinophils in ICAM-2$^{-/-}$ mice compared to wild-type mice is 78% and the p-value is <0.001.

(B) Eosinophil numbers in the BAL of bone marrow reconstituted ICAM-2$^{-/-}$ mice on day 21, 3 hr after OVA treatment. ICAM-2$^{-/-}$ mice with normal hematopoietic cells were generated by bone marrow transplantation. After challenge with OVA or PBS, the number of eosinophils in the BAL was determined. The average number of eosinophils in ICAM-2$^{-/-}$ recipient mice (KO; closed circle; PBS: n = 3; OVA: n = 9) is reduced by 76% compared to wild-type recipients (WT, open circle; PBS: n = 3; OVA: n = 5) and the p-value is <0.005.

(C) Comparison of eosinophil transmigration across ICAM-2$^{-/-}$ and wild-type endothelial cells. Numbers of eosinophils that transmigrated across wild-type (WT, bEND5; white bars) and ICAM-2-deficient (KO, bENDI2.3; gray bars) endothelial cells, which were either unstimulated (–) or TNFα-stimulated (+), are shown for one representative experiment out of four. Bars represent the mean (± SD) of six wells.

well as the inflammatory cytokines TNFα and IL-1α, were similar in mutant and wild-type mice throughout the OVA treatment (see Experimental Procedures; data not shown). These results were confirmed by RNase protection assays (RPA) in which mRNA levels of the cytokines IL-4, IL-5, TNFα, IL-1α, and IFNγ were tested in lung tissue from OVA-treated ICAM-2$^{-/-}$ mice and wild-type control mice (data not shown).

To determine whether ICAM-2 expression on T lymphocytes and/or other leukocyte subsets, which might regulate eosinophilia, is sufficient to restore eosinophil accumulation in the lung of ICAM-2$^{-/-}$ mice during an allergic inflammation, we replaced the entire hematopoietic system of ICAM-2$^{-/-}$ mice with wild-type cells using bone marrow transplantation. On day 21, 3 hr after OVA treatment, eosinophil numbers in the BAL of ICAM-2$^{-/-}$ mice transplanted with wild-type bone marrow were still 76% lower as compared to reconstituted wild-type control mice (Figure 2B). The engraftment efficiency in ICAM-2$^{-/-}$ and control mice was monitored by Southern blot analysis of genomic spleen DNA using a male specific hybridization probe (data not shown). The chimerism was 80%–100% in 19 out of 20 engrafted animals.

After we had established that ICAM-2-dependent eosinophil accumulation in the BAL is controlled by nonhematopoietic cells, we specifically studied the role of endothelial ICAM-2 expression in regulating transendothelial eosinophil migration. Endothelial cell lines from ICAM-2$^{-/-}$ and wild-type mice (brain-derived endothelioma ICAM-2$^{-/-}$ line 3 [bENDI2.3] and bEND5, respectively; see Experimental Procedures) were generated and migration of wild-type eosinophils through both types of endothelial cells was tested in an in vitro transendothelial migration assay. Significantly fewer eosinophils transmigrated through ICAM-2$^{-/-}$ endothelium than through normal endothelial cells (37% reduction; Figure 2C). Endothelial stimulation with TNFα induced upregulation of ICAM-1 and VCAM-1 on wild-type and ICAM-2$^{-/-}$ endothelial cells (data not shown) and led to a slight increase in transmigration through both types of endothelium (41% and 25% increase in transmigration through wild-type and ICAM-2$^{-/-}$ endothelial cells, respectively; Figure 2C).

Delayed but Not Abrogated Eosinophil Accumulation in the Airway Lumen of ICAM-2$^{-/-}$ Mice

To test if the observed reduction in transmigration through ICAM-2$^{-/-}$ endothelium causes a delay in eosinophil accumulation in the airway lumen or abolishes it completely, we examined BAL leukocyte numbers 1, 3, 6, 12, and 72 hr after OVA challenge on day 21 (Figure

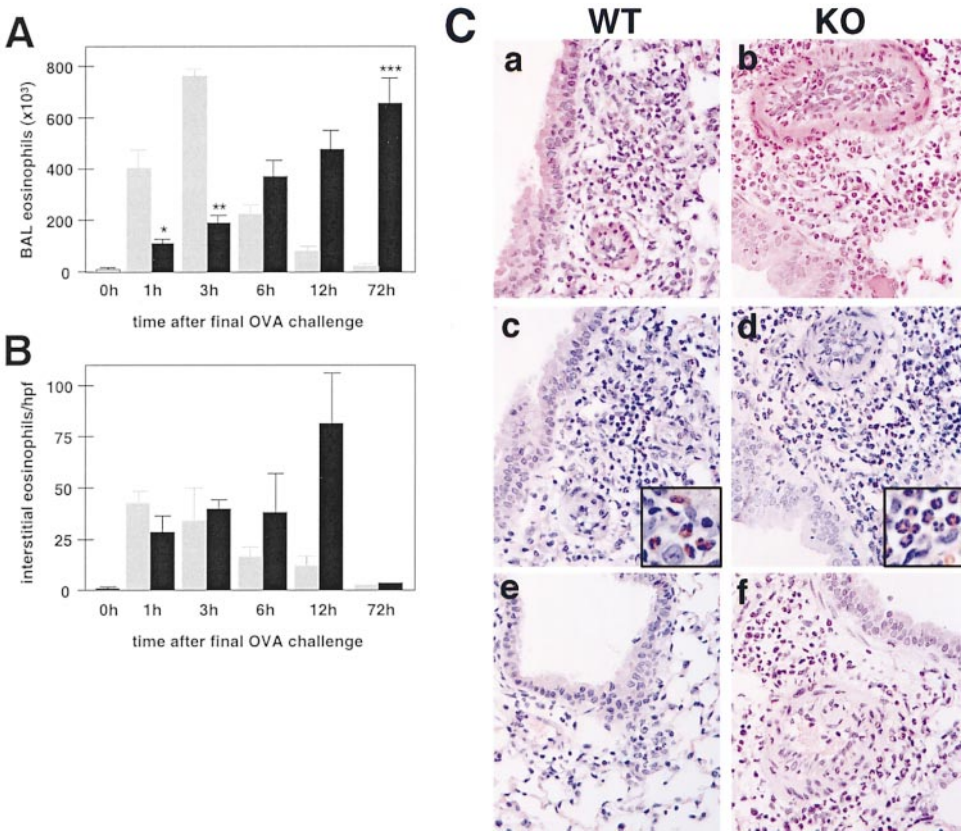

Figure 3. Eosinophil Presence in the Airway Lumen Is Delayed and Eosinophil Accumulation in Lung Tissue Is Prolonged in ICAM-2$^{-/-}$ Mice after OVA Treatment

(A) Time course of eosinophil accumulation in the airway lumen. Eosinophil numbers in BAL of wild-type mice (gray bars) and ICAM-2$^{-/-}$ mice (black bars) were determined 1, 3, 6, 12, and 72 hr after OVA challenge on day 21 and in untreated mice (0 hr). Bars represent the mean (± SEM) of five mice per group (*$p < 0.05$; **$p < 0.005$; ***$p < 0.005$).

(B) Enumeration of eosinophils in lung tissue. To determine the relative eosinophilia in wild-type (gray bars) and ICAM-2$^{-/-}$ mice (black bars) following OVA challenge, the total number of eosinophils in peribronchiolar fields was counted in five fields of H&E stained sections per mouse at a magnification of ×400. Bars represent the mean number (± SEM) of eosinophils per field for each group of mice ($n = 5$). The p-value at 12 hr is 0.065.

(C) Assessment of eosinophil activation in lung tissue sections. H&E staining of eosinophil morphology (a and b) and peroxidase staining of eosinophil granules (c–f) were performed in paraffin-fixed sections of lungs isolated from wild-type (WT) and ICAM-2$^{-/-}$ mice (KO). Panels a–d show staining of lung sections collected 3 hr after OVA challenge (magnification ×400). EPO staining of eosinophil granules resulted in a brown reaction product (insets in panels c and d). Panels e and f are photographs of EPO stained lung sections collected at 12 hr.

3A). As seen in previous experiments, BAL eosinophil numbers in wild-type mice reached their maximum 3 hr after OVA treatment and were back to normal levels at 12 hr. In ICAM-2$^{-/-}$ mice, eosinophil accumulation in the airway lumen was not abrogated but greatly delayed. BAL eosinophil numbers in ICAM-2$^{-/-}$ mice increased very slowly and reached levels comparable to those of wild-type mice only after 72 hr. Accumulation of lymphocytes and monocytes in the airway lumen was not significantly delayed in ICAM-2$^{-/-}$ mice and was highest 3 hr after antigen treatment (data not shown).

Prolonged Presence of Eosinophil Infiltrates in Lung Tissue of ICAM-2$^{-/-}$ Mice after OVA Treatment

To determine whether the delayed eosinophil accumulation in the airway lumen was due to slower endothelial transmigration in vivo, we assessed the extent of leukocyte migration to the lung interstitium. Hematoxylin and eosin (H&E) stained lung sections from OVA-treated mice revealed the presence of substantial interstitial infiltrates in perivascular and peribroncheolar areas in wild-type mice as soon as 1 hr after OVA challenge (relative histological scores [± SEM] of 3 [± 0.3] and 2.8 [± 0.6] at 1 hr and 3 hr, respectively). In ICAM-2$^{-/-}$ mice, numbers of interstitial infiltrates increased more slowly and reached their maximum only 3 hr after antigen challenge (scores of 2.5 [± 0.5] and 3.6 [± 0.3] at 1 hr and 3 hr, respectively). While the number of infiltrates started to decrease in wild-type mice 6 hr after OVA treatment (scores of 2.3 [± 0.6], 1.8 [± 0.4], and 2.1 [± 0.9] at 6 hr, 12 hr, and 72 hr, respectively), interstitial infiltrates in ICAM-2$^{-/-}$ mice were not reduced until 72 hr after antigen challenge (scores of 3.2 [± 0.5], 3.2 [± 0.5], and 2.3 [± 0.8] at 6 hr, 12 hr, and 72 hr, respectively].

Closer examination of the infiltrate composition revealed that eosinophil numbers in the interstitium paralleled the number of infiltrates (Figure 3B). In the interstitium of wild-type mice, eosinophil accumulation

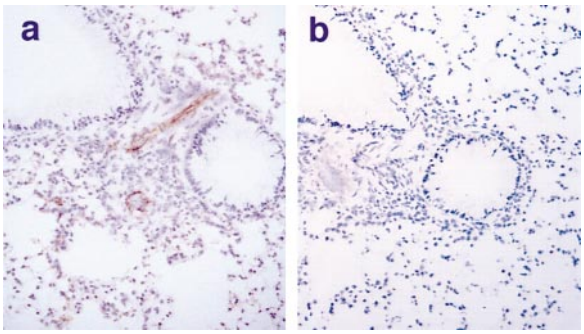

Figure 4. ICAM-2 Expression in Lung Tissue Is Not Altered after OVA Treatment

The distribution of ICAM-2 protein in wild-type lungs following OVA treatment was determined by immunohistochemical staining of frozen sections with α-ICAM-2 MAb (a) and a negative control antibody (b) (magnification ×200).

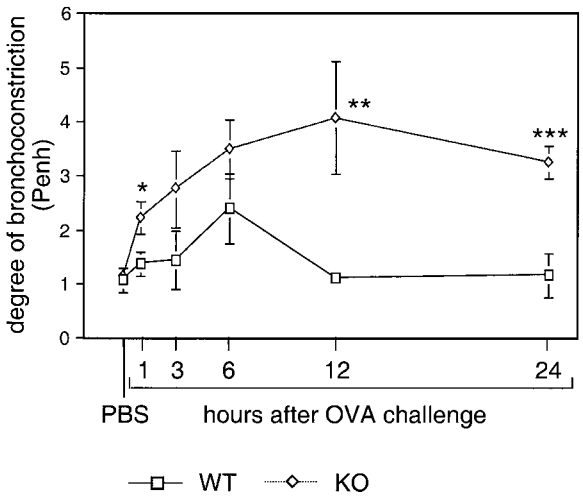

Figure 5. Prolonged Airway Hyperresponsiveness in ICAM-$2^{-/-}$ Mice

The degree of bronchoconstriction was measured in wild-type (WT, squares) and ICAM-$2^{-/-}$ mice (KO, diamonds) 1, 3, 6, 12, and 24 hr after the last OVA or PBS challenge on day 21. Mice were exposed to an aerosol of methacholine (80 mg/ml) for 1 min and airway constriction was evaluated for the next 5 min. Results are shown as mean (± SEM) of Penh for n = 5 mice per time point (*$p < 0.05$; **$p < 0.05$; ***$p < 0.01$).

reached a maximum as early as 1 hr after antigen challenge and started to decrease at 6 hr. In ICAM-$2^{-/-}$ mice, maximal eosinophil numbers in the interstitium, which were approximately 100% higher than the maximal eosinophil numbers detected in wild-type interstitium at 1 hr, were observed 12 hr after OVA treatment. The observed time course of eosinophil accumulation in the interstitium also paralleled changes in eosinophil numbers in the airway lumen as enumerated by BAL (Figure 3A). Complementary eosinophil distribution between the two compartments was demonstrated at 72 hr in ICAM-$2^{-/-}$ mice, when eosinophils were no longer detectable in the interstitium, but reached a corresponding maximum in BAL.

Differences in numbers as well as activation/degranulation of eosinophils between wild-type and ICAM-$2^{-/-}$ mice were assessed by morphological staining (H&E) and cyanide-resistant eosinophil peroxidase (EPO) staining of eosinophils in serial sections of OVA-treated lungs (Figure 3C). Three hours after OVA treatment, equivalent numbers of eosinophils were detected by morphological staining (Figures 3Ca and 3Cb) and peroxidase staining of granules (Figures 3Cc and 3Cd) in wild-type and ICAM-$2^{-/-}$ mice, which indicates that eosinophils in wild-type and mutant mice do not overtly differ in their activation/degranulation status. At 12 hr after OVA treatment, both EPO and H&E staining of lung sections revealed widespread eosinophil infiltration in ICAM-$2^{-/-}$ mice but only small infiltrates in wild-type mice (Figures 3Ce and 3Cf; data not shown).

We studied possible correlations between the phenotype observed in ICAM-$2^{-/-}$ mice (delayed eosinophil accumulation in the airway lumen and prolonged presence of eosinophils in lung interstitium) and the pattern of ICAM-2 expression in inflamed lung. High expression of ICAM-2 on lung vascular endothelium and in alveolar walls was observed before and after OVA treatment by immunohistochemical staining of tissue sections (Figures 1C and 4). Additional ICAM-2 expression was identified in some cell clusters in the mononuclear infiltrates. Little, if any, ICAM-2 expression was observed with this method on large airway epithelium, before or after OVA treatment.

We investigated quantitative changes in ICAM-2 expression in whole lung tissue upon OVA treatment using cDNA microarray technology. Hybridization of an ICAM-2 DNA fragment containing microarray with cDNA from untreated as well as OVA-treated wild-type lungs revealed a 3.5-fold upregulation of ICAM-2 expression upon OVA treatment (data not shown).

Prolonged Airway Hyperresponsiveness in ICAM-$2^{-/-}$ Mice

To evaluate if the prolonged and increased accumulation of eosinophils in lung interstitium and the delayed presence of eosinophils in the airway lumen causes changes in airway BHR, we measured bronchoconstriction in response to methacholine (Mch) provocation in OVA-treated mice (Figure 5). BHR was increased in wild-type and mutant mice as early as 1 hr after antigen treatment and reached its maximum at 6 hr in wild-type mice. While airway hyperresponsiveness returned to baseline levels in wild-type mice 12 hr after OVA challenge, BHR remained high in ICAM-$2^{-/-}$ mice. In fact, ICAM-$2^{-/-}$ mice were hyperresponsive for at least another 48 hr (Figure 5; data not shown). At all time points studied, an overall increase in BHR was observed in ICAM-$2^{-/-}$ mice as compared to wild-type mice.

In Vivo Homing of Lymphocytes in ICAM-$2^{-/-}$ Mice

To test if ICAM-2 deficiency affects lymphocyte migration to lymph nodes (LN), we traced the in vivo homing of fluorescently labeled LN cells to peripheral LN, mesenteric LN, and spleen. In the representative experiment shown in Figure 6, the absolute numbers of peripheral LN cells from ICAM-$2^{-/-}$ and wild-type mice, which homed to peripheral and mesenteric LN, Peyer's patches, and

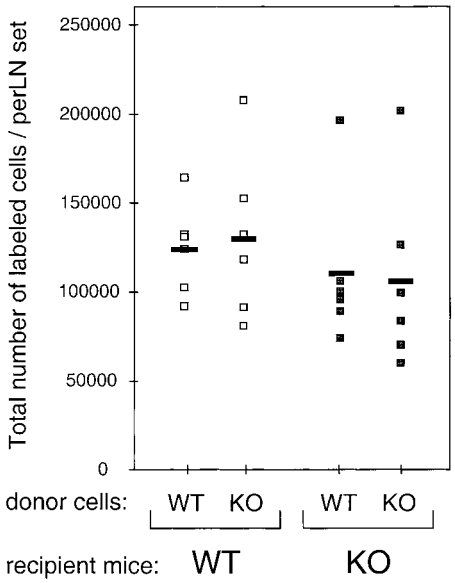

Figure 6. Lymphocyte Homing Is Not Affected by the Lack of ICAM-2 Expression

The homing of wild-type and ICAM-2$^{-/-}$ lymphocytes to peripheral LN of wild-type (WT) and ICAM-2$^{-/-}$ mice (KO) in the resting state was tested 90 min after injection of donor cells from peripheral LN. Each square represents the total number of either TRITC-labeled wild-type or Calcein-AM-labeled ICAM-2$^{-/-}$ donor cells detected in the peripheral LN sets of a single recipient mouse, which has either wild-type (WT; white squares) or ICAM-2$^{-/-}$ (KO; gray squares) genotype. Bars represent the mean of each group (n = 6).

the spleen (Figure 6; data not shown) in wild-type and ICAM-2$^{-/-}$ recipient mice are not significantly different. Labeled wild-type cells (± SEM) represented 0.44% (± 0.03%) and 0.45% (± 0.04%) of peripheral LN cells, 0.50% (± 0.05%) and 0.44% (± 0.06%) of mesenteric LN cells, and 0.17% (± 0.01%) and 0.18% (± 0.02%) of Peyer's patch cells in normal and ICAM-2$^{-/-}$ recipient mice, respectively. Likewise, the lack of ICAM-2 expression on injected lymphocytes from ICAM-2$^{-/-}$ mice did not alter their ability to home to the respective organs (0.46% [± 0.06%] and 0.44% [± 0.07%] in peripheral LN, 0.42% [± 0.05%] and 0.35% [± 0.05%] in mesenteric LN, and 0.15% [± 0.01%] and 0.15% [± 0.01%] in Peyer's patch cells of wild-type and ICAM-2 deficient mice, respectively). These data were confirmed by the observation that B and T lymphocyte and myeloid cell subpopulations were equally distributed in LN and Peyer's patches of resting ICAM-2$^{-/-}$ and wild-type mice (data not shown).

Discussion

The results reported here demonstrate that ICAM-2 plays a critical role in eosinophil trafficking and localization within the lung tissue during lung allergic inflammation. These data also highlight the importance of eosinophil localization for the development and maintenance of BHR.

The data presented in this manuscript raise two points for further discussion: (1) which molecular mechanisms underlie the prolonged accumulation of eosinophils in lung interstitium and their delayed appearance in the airway lumen; and (2) what are the physiological consequences of this abnormal redistribution of eosinophils for airway function?

With respect to the first issue, ICAM-2 could control eosinophil accumulation in the airway lumen by the following mechanisms: (1) by directly mediating adhesive interactions of eosinophils with components of the lung, (2) indirectly, by controlling the recruitment of other leukocyte subsets to the inflammatory site, (3) by regulating the expression and release of activating cytokines and chemokines, or (4) by regulating eosinophil development and release from the bone marrow. Here, we show that ICAM-2 controls eosinophil accumulation in the airway lumen by direct adhesive interactions. We demonstrate that in ICAM-2$^{-/-}$ mice, T lymphocyte, monocyte, and macrophage numbers in the lung are not significantly reduced (Figure 2A), and levels of cytokines are not overtly altered (data not shown). Furthermore, we show that eosinophil numbers in peripheral blood and bone marrow are not reduced in the mutant mice (data not shown), indicating that ICAM-2 expression on early hematopoietic progenitor cells and bone marrow endothelium is not essential for eosinophil development and release from the bone marrow.

Using bone marrow chimeras (Figure 2B), we demonstrate unequivocally that these critical adhesive interactions are not mediated by ICAM-2 expressed on eosinophils or other leukocytes, but rather by ICAM-2 expressed on non-bone marrow–derived cells, presumably on lung resident cells. ICAM-2 expression in lung tissue seems to be restricted to vascular endothelium, which shows high expression of ICAM-2, and to alveolar walls (Figures 1C and 5). In large airway epithelium, ICAM-2 expression is detectable neither before nor after OVA treatment. However, we cannot exclude that ICAM-2 is expressed on airway epithelium at levels that are not detectable by immunohistochemistry. The observed upregulation of ICAM-2 mRNA expression in whole lung tissue upon OVA treatment could further support the requirement of ICAM-2-mediated adhesive interactions during this inflammatory response.

Our observation that eosinophil accumulation in the airway lumen, as monitored by BAL, was delayed in ICAM-2$^{-/-}$ mice suggests that ICAM-2 specifically controls the exit of eosinophils to the airway lumen by mediating epithelial and/or endothelial transmigration of eosinophils. The histological analysis of lung tissue at various time points after OVA treatment revealed that the kinetics of eosinophil accumulation in airway interstitium complements that of eosinophil accumulation in the airway lumen. While eosinophil infiltrates were comparable 3 hr after OVA treatment in wild-type and mutant mice, they developed more slowly and persisted much longer in the interstitium of ICAM-2$^{-/-}$ mice as compared to control mice. Eosinophil infiltrates were most prominent at 12 and 24 hr after antigen challenge in ICAM-2-deficient mice, whereas in wild-type mice infiltrates were almost completely resolved at the same time points. By 72 hr, eosinophils are no longer found in the lung interstitium but are still detectable in the airway lumen of ICAM-2$^{-/-}$ mice (Figure 3; data not shown). Therefore,

we propose that ICAM-2 expressed on vascular endothelium, alveolar walls, and possibly large airway epithelium mediates the trafficking of eosinophils through interstitium and their exit to the lumen of the airways. Control of endothelial eosinophil transmigration by ICAM-2 expression was confirmed using an in vitro transendothelial migration assay in which eosinophils transmigrate normally through wild-type endothelium, but eosinophil transmigration through ICAM-2$^{-/-}$ endothelium derived from the mutant mice is greatly reduced (Figure 2C). The role that ICAM-2 plays in transepithelial migration is being evaluated at present using a transepithelial chemotaxis assay.

The second aspect highlighted by the findings reported here is the effect on lung function of the prolonged eosinophil accumulation in the lung interstitium. Airway BHR, a major characteristic of allergic asthma, is induced by eosinophils that secrete toxic granular proteins that cause airway damage and smooth muscle contractility. The BHR response in ICAM-2$^{-/-}$ mice, like in wild-type littermates, developed early after OVA treatment and increased further until 6 hr after antigen challenge (Figure 5). While BHR returned to baseline levels 12 hr after antigen challenge in wild-type mice, it increased further in ICAM-2$^{-/-}$ mice, which indicates that the specific location of eosinophils within the lung is critical for their deleterious effects. In fact, increased BHR in ICAM-2$^{-/-}$ mice could be demonstrated 24 and 48 hr after OVA challenge (Figure 5; data not shown), time points at which numbers of eosinophils in the lung interstitium of mutant mice were still increased. Eosinophils that accumulated in the lung interstitium, but not the eosinophils in the airway lumen, seem to be mostly responsible for the induction/development of BHR. This interpretation is supported by the observation that the recruitment of eosinophils to the airway lumen alone does not induce BHR, and that the development of BHR depends on the localization of eosinophils in the submucosa of the bronchial epithelium [Eum et al., 1995]. Furthermore, these results correlate well with our previous observation, that mice showing reduced interstitial eosinophilia, but unaffected BAL eosinophilia after blockage of the chemokine MCP-5, did not develop BHR (Gonzalo et al., 1998). Likewise, a recent clinical study (Crimi et al., 1998) has found no significant correlations between the degree of BHR and the numbers of inflammatory cells in sputum or BAL or bronchial biopsy. In contrast, correlations have been established between the number of eosinophils in the BAL of patients and the severity of disease (Azzawi et al., 1990; Howarth et al., 1994; Djukanovic, 1996). Our study demonstrates that lengthened BHR correlates well with the prolonged presence of eosinophils in the interstitium and does not correlate with the peak of eosinophil accumulation in the airway lumen.

We could not detect differences between the interstitial infiltrates of ICAM-2$^{-/-}$ and wild-type mice when eosinophils were identified based on either granule content or morphology (Figure 3C). This finding supports the concept that ICAM-2 controls eosinophil localization rather than eosinophil activation (i.e., cell granule content; Lefort et al., 1996; Evans et al., 1997), and that the localization of eosinophils in lung tissue is essential for the development of BHR.

Although time windows of BHR vary dramatically in different models of lung allergic inflammation (Eum et al., 1995; Foster et al., 1996; Gonzalo et al., 1996a; Hamelmann et al., 1996), the underlying reasons for these differences have not been elucidated. Instead, the rather different phenotypes have been interpreted based on the use of mice with different genetic backgrounds, protocols of immunization, antigens, etc. Here, we describe a single gene defect that dramatically prolongs BHR in mice. This is of critical importance since time windows of hyperresponsiveness in asthmatic patients correlate directly with disease progression and quality of life.

The impaired migration of eosinophils during lung allergic inflammation contrasts with the unaltered lymphocyte homing to lymph nodes (Figure 6). This is an important observation, since ICAM-2 had been postulated to be a critical adhesion receptor controlling steady state recirculation of lymphocytes, based on in vitro studies and its high constitutive expression on high endothelial venules (Springer, 1994). Results presented here show that this is not the case in vivo.

A number of other phenotypical aspects have been examined in these ICAM-2$^{-/-}$ mice and are summarized in Table 1. This summary does not represent a detailed characterization of the phenotypes but is rather intended to serve as a reference guide for investigators in the field. Of special notice is the reduction of megakaryocyte progenitors in the bone marrow of ICAM-2$^{-/-}$ mice. The complete characterization of this finding will be presented elsewhere.

In conclusion, our findings establish a critical role for ICAM-2 in the distribution of eosinophils between the lung interstitium and airway lumen during the development of allergic lung inflammation. Furthermore, we have established, using a clean genetic system, that the localization of eosinophils within the lung interstitium is key for the induction/development of BHR. These results clearly demonstrate that ICAM-2 is not the major mediator of lymphocyte homing in the resting state as anticipated but plays an essential role in eosinophil trafficking within the lung during an allergic inflammatory response.

Experimental Procedures

Generation of ICAM-2-Deficient Mice

The ICAM-2 gene targeting vector was constructed using a 6.3 kb XbaI fragment of genomic DNA that had been isolated from an AKR mouse strain genomic library (Xu et al., 1992). This DNA fragment, containing exons 1 and 2, was subcloned in pBlueScript (KS). A 1.7 kb EcoRI–HindIII fragment carrying a polyadenylated *neomycin resistance* gene (*neo*-polyA+) under the control of the *phosphoglycero kinase* gene (PGK) promoter (a gift from Drs. E. Li and R. Jaenisch, Massachusetts Institute of Technology, Cambridge, MA) was isolated from pKJ1 (Li et al., 1992) and blunted with Klenow. This fragment was inserted into the blunted NdeI site in the second exon of the ICAM-2 gene in the 6.3 kb fragment. In parallel, a 2.7 kb EcoRI–HindIII fragment of pGEM7 (*thymidin kinase* [*tk*]) containing the HSV*tk* gene under the control of the PGK promoter was subcloned in pBlueScript (KS). Finally, the 8.0 kb XbaI fragment of ICAM-2 containing the *neo* insert was subcloned into the XbaI site of the pBlueScript (KS) vector containing the *tk* gene.

The linearized plasmid was used to transfect J1 ES cells, obtained from Drs. E. Li and R. Jaenisch, as described (Li et al., 1992). Recombinant clones were identified by Southern blot analysis of BamHI digested DNA using a 3′ flanking probe containing exons 3 and 4 (Figure 1A) and a specific *neo*^{r} gene fragment. Homologous recombination was observed with a frequency of 1 in 4.5 resistant clones.

Embryo manipulations and backcrosses of chimeras to C57BL/6 mice were performed as described (Bradley, 1987; Li et al., 1992).

Leukocyte Isolation, Counts, Antibody Staining, and FACS Analysis

Blood leukocytes were obtained by cardiac puncture, and complete blood cell counts were determined using an H*1E Automated Analyzer (Technicon, Bayer Corp.). Single cell suspensions from inguinal, axillary, and cervical LN (peripheral LN), mesenteric LN, bone marrow, spleen, and thymus were prepared, erythrocytes were lysed, and cell numbers were determined using a hemocytometer. For three- color flow cytometry, cells were first preblocked with purified α-mouse Fc receptor antibody (α-CD16/32; 2.4G2) from PharMingen (San Diego, CA). Cells were stained with antibodies directly conjugated with fluorochrome: α-B220 (RA3-6B2), α-IgM (G155-228), α-TCRβ (H57-597), α-Thy-1.2 (53-2.1), α-CD4 (L3T4), α-CD8 (53-6.7), α-Mac-1 (M1/70), α-Gr-1 (RB6-8C5), α-ICAM-1 (3E2), and irrelevant isotype controls from PharMingen. ICAM-2 staining was done using either fluorochrome-labeled α-ICAM-2 MAb (IC2-3C4; Xu et al., 1996] from PharMingen or unlabeled α-ICAM-2 MAb kindly provided by Z. Awdeh (Center for Blood Research, Boston, MA) and fluorochrome-labeled α-rat IgG2a,K MAb from PharMingen as secondary antibody. Dead cells were excluded by staining with propidium iodide (1 μg/ml final concentration). Samples were analyzed using a FACScan instrument (Becton Dickinson and Co., Mountain View, CA).

Immunohistochemical Analysis of ICAM-2 Expression

Fixed cryosections (4 μm) of wild-type and ICAM-2$^{-/-}$ mouse tissues were stained with rat monoclonal antibodies directed against ICAM-2 (PharMingen) using an avidin/biotin staining method as previously described (Gonzalo et al., 1996b). The following control slides were included: (1) stained with an isotype-matched negative control antibody instead of α-ICAM-2 antibody, (2) omission of biotinylated α-rat immunoglobulin, or (3) omission of streptavidin complex. All slides were counterstained with hematoxylin.

NK Cell Cytotoxicity and LAK Assay

The endogenous NK cell cytotoxicity was determined by measuring NK-mediated cytotoxic lysis of YAC-1 target cells using a standard ^{51}Cr release assay (Wang et al., 1994). All mice were injected i.p. with 100 μg poly I:C 16–24 hr before being sacrificed. LAK cell activity was assessed by overnight culture of the spleen cells (1×10^7/ml) with mIL-2 (300 U/ml; Genzyme) followed by the standard ^{51}Cr release assay (Wang et al., 1994).

CFU-GM and Megakaryocyte Progenitor Assays

For CFU-GM assays, appropriate numbers of bone marrow, spleen, and peripheral blood cells from individual mice were plated in methylcellulose as described (Schmits et al., 1997).

CFU-MK and single cell megakaryocyte growth assays were performed as previously described (Banu et al., 1995). In each experiment, bone marrow from two mice was pooled.

Platelet Assays

Platelet numbers were determined using a hemocytometer. Thrombocytopenia was induced by injection of 5-fluorouracil (FU; Sigma, St. Louis, MO; 150 mg/kg i.v.) and platelet recovery was assessed by platelet counts on days 3, 7, and 14.

For measurement of bleeding times in unanesthesized mice, 2 mm of the tail tip were cut off and the tail was placed in isotonic saline at 37°C immediately after injury. Bleeding times were measured from the moment the tail was cut until bleeding stopped completely.

Mouse Model of Lung Inflammation

The mouse model of lung inflammation has been previously described (Gonzalo et al., 1996a). Among the BAL cells, T lymphocytes, B lymphocytes, and mononuclear phagocytes were identified by Thy1.2 (53-2.1) (PharMingen, San Diego, CA), IgM (II/41) (PharMingen, San Diego, CA), and Moma-2 (Biosource Int. Camarillo, CA) staining, respectively, of BAL cell cytospins (Gonzalo et al., 1996b).

To determine eosinophil numbers in bone marrow and peripheral blood after OVA treatment, equivalent numbers of leukocytes were pelleted onto glass slides by cytocentrifugation and stained using a sensitive method dependent on the presence of cyanide-resistant peroxidase (Boyce et al., 1995). The percentage of eosinophils, lymphocytes, monocytes, and macrophages was determined by counting their number in eight high-power fields (×400 magnification; total area 0.5 mm^2) per area randomly selected and dividing this number by the total number of cells per high-power field. To obtain the absolute number of each leukocyte subtype in the lavage, these percentages were multiplied by the total number of cells recovered from the BAL fluid.

Lung sections from the different experimental groups of mice were prepared as described (Gonzalo et al., 1996b). Sizes of pulmonary infiltrates were assessed and scored using a semiquantitative system. Sections were graded from "0"—where no infiltrating cells were observed, to "+5"—where all vessels and bronchioles were surrounded by leukocytic infiltrate of at least three cells deep. Eosinophils were counted in H&E stained sections by determining the number of eosinophils per peribronchiolar field at a magnification of ×400 in five fields per mouse. All sections were coded and scored blind by at least two observers. Eosinophil granules were detected using the EPO staining method (Boyce et al., 1995).

ELISA, RPA, and cDNA Microarrays

Cytokine levels were determined on day 16, 1 hr, and on day 21, 3 hr after OVA treatment in the BAL fluid using commercial ELISA kits (Endogen, Cambridge, MA).

At the same time points, cytokine mRNA levels in total lung RNA were analyzed using a RiboQuant RPA kit (PharMingen) as recommended by the supplier.

ICAM-2 expression levels in untreated and OVA-treated lungs (day 21, 3 hr) were compared using the cDNA microarray technology as previously described (Nguyen et al., 1995).

Bone Marrow Transplantation Experiments

Lethally irradiated female ICAM-2$^{-/-}$ and wild-type mice received 5×10^6 bone marrow cells from male wild-type control mice by i.v. injection. After a recovery period of 5 weeks, the engrafted mice were OVA treated and BAL fluid was analyzed on day 21, 3 hr after the last OVA challenge.

The engraftment efficiency was assessed by Southern blot analysis of genomic spleen DNA (10 μg) using the male specific pY2 hybridization probe (Bernad et al., 1994), kindly provided by Dr. A. Bernad (Universidad Autonoma, Madrid, Spain). The intensity of the male specific signal in each lane was determined by densitometric analysis. Control lanes for quantitation were loaded with graded mixtures of male and female genomic spleen DNA (10 μg total).

Generation of Endothelial Cell Lines and Transmigration Assays

Endothelial cell lines were isolated from ICAM-2$^{-/-}$ mice as previously described for the wild-type line bEND5 (Röhnelt et al., 1997). For activation studies, endothelioma cell lines were stimulated with 5 nM recombinant murine TNFα (Bioconcept, Umkirch, Germany) as indicated.

Transmigration assays were performed as previously described (Röhnelt et al., 1997) using 6.5 mm Transwells (Costar, Bodenheim, Germany) with 5 μm pore size. Inserts were coated with laminin (Boehringer Mannheim, Mannheim, Germany; 50 μg/ml). 3×10^5 endothelioma cells were seeded on top of each porous filter and cultured for 2 days. On day 3, eosinophils were added on top of each filter and the assays were run for 2 hr at 37°C and 10% CO_2. The 2 hr time point was chosen as it was the earliest time point that allowed us to harvest enough transmigrated eosinophils to perform comparative studies. Migrated eosinophils were collected for cell counting and analyzed microscopically in Pappenheim-stained cytospins and by FACS analysis. Confluency of the endothelial monolayer was confirmed after each assay by Giemsa staining of inserts. Assays were performed as triplicates for each value.

Evaluation of Bronchoconstriction

The degree of bronchoconstriction was measured 1, 3, 6, 12, 24, and 48 hr after the last antigen challenge by recording respiratory

pressure curves by whole body plethysmography (Buxco Technologies, Niskayuna, NY) in response to inhaled methacholine (Mch, Aldrich, Milwaukee, WI) at a concentration of 80 mg/ml for 1 min, as described previously (Eum et al., 1995; Tsuyuki et al., 1997). BHR was expressed as enhanced pause (Penh), a calculated value, which correlates with measurement of airway resistance, impedance, and intrapleural pressure in the same mouse. Penh = (Te/Tr-1) × (Pef/Pif) (Te, expiration time; Tr, relaxation time; Pef, peak expiratory flow; Pif, peak inspiratory flow × 0.67 = coefficient) (Gelfand and Irvin, 1997). The relaxation time is the time it takes for the box pressure to change from a maximum to a user-defined percentage of the maximum. Here, Tr measurement began at the maximum box pressure and ended at 40%.

In Vivo Lymphocyte Homing Assays

For resting state lymphocyte homing assays, peripheral LN cell suspensions from mutant and wild-type mice were labeled with two different fluorescent dyes, tetramethyl rhodamine isothiocyanate (TRITC) and calcein-acetoxymethyl ester (Calcein-AM), as previously described (Martin and Miller, 1989). An equimolar mixture of both lymphocyte populations (1×10^7 cells each) was injected i.v. into both ICAM-$2^{-/-}$ mice and littermate controls. 90 min later, the mice were sacrificed and the total number of labeled cells in single-cell suspensions of peripheral LN sets, mesenteric LN, and Peyer's patches was determined by flow cytometry.

Acknowledgments

The authors are indebted to W. N. Khan for his advice on the ES cell work, to S. Schieferl and R. Kulbacki for blastocyst injections, to G. Hoch for excellent technical assistance, and to E. R. Unanue, A. K. Abbas, E. C. Butcher, R. P. Schleimer, J. M. Drazen, and G. I. Kingsbury for critical reading of this manuscript. N. G. was a recipient of a postdoctoral fellowship of the Deutsche Forschungsgemeinschaft.

Received April 21, 1998; revised November 24, 1998.

References

Arnaout, M.A. (1990). Structure and function of the leukocyte adhesion molecules CD11/CD18. Blood *75*, 1037–1050.

Azzawi, M., Bradley, B., and Jeffery, P.K. (1990). Identification of activated T-lymphocytes and eosinophil in bronchial biopsies in stable atopic asthmatics. Am. Rev. Respir. Dis. *142*, 1407–1413.

Banu, N., Wang, J.F., Deng, B., Groopman, J.E., and Avraham, H. (1995). Modulation of megakaryocytopoiesis by thrombopoietin: the c-Mpl ligand. Blood *86*, 1331–1338.

Bernad, A., Varas, F., Gallego, J.M., Almendral, J.M., and Bueren, J.A. (1994). Ex vivo expansion and selection of retrovirally transduced bone marrow: an efficient methodology for gene-transfer to murine lympho-haemopoietic stem cells. Br. J. Hematol. *87*, 6–17.

Boyce, J.A., Friend, D., Matsumoto, R., Austen, K.F., and Owen, W.F. (1995). Differentiation in vitro of hybrid eosinophil/basophil granulocytes: autocrine function of an eosinophil developmental intermediate. J. Exp. Med. *182*, 49–57.

Bradley, A. (1987). Production and analysis of chimaeric mice. In Teratocarcinomas and Embryonic Stem Cells: A Practical Approach, E.J. Robertson, ed. (Oxford, England: IRL Press at Oxford University Press), pp. 113–151.

Butcher, E.C. (1991). Leukocyte-endothelial cell recognition: three (or more) steps to specificity and diversity. Cell *67*, 1033–1036.

Cockcroft, D.W., Killian, D.N., Mellon, J.J., and Hargreave, F.E. (1977). Bronchial reactivity to inhaled histamine: a method and clinical survey. Clin. Allergy *7*, 235–243.

Connolly, E.S., Winfree, C.J., Springer, T.A., Naka, Y., Liao, H., Yan, S.D., Stern, D.M., Solomon, R.A., Gutierrez-Ramos, J.C., and Pinsky, D.J. (1996). Cerebral protection in homozygous null ICAM-1 mice after middle cerebral artery occlusion. Role of neutrophil adhesion in the pathogenesis of stroke. J. Clin. Invest. *97*, 209–216.

Crimi, E., Spanevello, A., Neri, M., Ind, P.W., Rossi, G.A., and Brusasco, V. (1998). Dissociation between airway inflammation and airway hyperresponsiveness in allergic asthma. Am. J. Respir. Crit. Care. Med. *157*, 4–9.

de Fougerolles, A.R., Stacker, S.A., Schwarting, R., and Springer, T.A. (1991). Characterzation of ICAM-2 and evidence for a third counter-receptor for LFA-1. J. Exp. Med. *174*, 253–267.

de Fougerolles, A.R., and Springer, T.A. (1992). Intercellular adhesion molecule *3*, a third adhesion counter-receptor for lymphocyte function-associated molecule 1 on resting lymphocytes. J. Exp. Med. *175*, 185–190.

Diacovo, T.G., de Fougerolles, A.R., Bainton, D.F., and Springer, T.A. (1994). A functional integrin ligand on the surface of platelets: intercellular adhesion molecule-2. J. Clin. Invest. *94*, 1243–1251.

Djukanovic, R. (1996). Bronchoscopy as a research tool for the study of asthma pathogenesis and effects of antiasthma drugs. J. Allergy Clin. Immunol. *98*, S41–S45.

Dustin, M.L., and Springer, T.A. (1988). Lymphocyte function associated antigen-1 (LFA-1) interaction with intercellular adhesion molecule-1 (ICAM-1) is one of at least three mechanisms for lymphocyte adhesion to cultured endothelial cells. J. Cell. Biol. *107*, 321–331.

Eum, S.-Y., Hailé, S., Lefort, J., Huerre, M., and Vargaftig, B.B. (1995). Eosinophil recruitment into the respiratory epithelium following antigenic challenge in hyper-IgE mice is accompanied by interleukin 5-dependent bronchial hyperresponsiveness. Proc. Natl. Acad. Sci. USA *92*, 12290–12294.

Evans, C.M., Fryer, A.D., Jacoby, D.B., Gleich, G.J., and Costello, R.W. (1997). Pretreatment with antibody to eosinophil major basic protein prevents hyperresponsiveness by protecting neuronal M_2 muscarinic receptors in antigen-challenged guinea pigs. J. Clin. Invest. *100*, 2254–2262.

Foster, P.S., Hogan, S.P., Ramsay, A.J., Matthaei, K.I., and Young, I.G. (1996). Interleukin 5 deficiency abolishes eosinophilia, airways hyperreactivity, and lung damage in a mouse asthma model. J. Exp. Med. *183*, 195–201.

Gelfand, E.W., and Irvin, C.G. (1997). T lymphocyte: setting the tone of the airways. Nat. Med. *3*, 382–383.

Gleich, G.J., Flavahan, N.A., Fujisawa, T., and Vanhoutte, P.M. (1988). The eosinophil as a mediator of damage to respiratory epithelium: a model for bronchial hyperreactivity. J. Allergy Clin. Immunol. *81*, 776–881.

Gonzalo, J.-A., Jia, G.-Q., Aguirre, V., Friend, D., Coyle, A.J., Jenkins, N.A., Lin, G.S., Katz, H., Litchman, A., Copeland, N., et al. (1996a). Mouse eotaxin expression parallels eosinophil accumulation during lung allergic inflammation but it is not restricted to a Th2-type response. Immunity *4*, 1–14.

Gonzalo, J.A., Lloyd, C.M., Kremer, L., Finger, E., Martinez-A, C., Siegelman, M.H., Cybulski, M., and Gutierrez-Ramos, J.C. (1996b). Eosinophil recruitment to the lung in a murine model of allergic inflammation: the role of T cells, chemokines and endothelial adhesion receptors. J. Clin. Invest. *98*, 2332–2345.

Gonzalo, J.A., Lloyd, C.M., Wen, D., Albar, J.P., Wells, T.N., Proudfoot, A., Martinez-A, C., Dorf, M., Bjerke, T., Coyle, A.J., and Gutierrez-Ramos, J.C. (1998). The coordinated action of CC chemokines in the lung orchestrates allergic inflammation and airway hyperresponsiveness. J. Exp. Med. *188*, 157–167.

Hamelmann, E., Oshiba, A., Paluh, J., Bradley, K., Loader, J., Potter, T.A., Larsen, G.L., and Gelfand, E.W. (1996). Requirement for $CD8^+$ T cells in the development of airway hyperresponsiveness in a murine model of airway sensitization. J. Exp. Med. *183*, 1719–1729.

Howarth, P.H., Bradding, P., Montefort, S., Peroni, D., Djukanovic, R., Carroll, M.P., and Holgate, S.T. (1994). Mucosal inflammation and asthma. Am. J. Respir. Crit. Care. Med. *150*, S18–S22.

Kelly, K.J., Williams, W.W., Colvin, R.B., Meehan, S.M., Springer, T.A., Gutierrez-Ramos, J.C., and Bonventre, J.V. (1996). Intercellular adhesion molecule-1-deficient mice are protected against ischemic renal injury. J. Clin. Invest. *97*, 1056–1063.

Kishimoto, T.K., Larson, R.S., Corbi, A.L., Dustin, M.L., Staunton, D.E., and Springer, T.A. (1989). The leukocyte integrins: LFA-1, Mac-1 and p150,95. Adv. Immunol. *46*, 149–182.

Lasky, L.A. (1992). Selectins: interpreters of cell-specific carbohydrate information during inflammation. Science *258*, 964–969.

Lefort, J., Nahori, M.-A., Ruffie, C., Vargaftig, B.B., and Pretolani, M. (1996). In vivo neutralization of eosinophil-derived major basic protein inhibits antigen-induced bronchial hyperreactivity in sensitized guinea pigs. J. Clin. Invest. *97*, 1117–1121.

Li, E., Bestor, T.H., and Jaenisch, R. (1992). Targeted mutation of the DNA methyltransferase gene results in embryonic lethality. Cell *69*, 915–926.

Martin, D.R., and Miller, R.G. (1989). In vivo administration of histocompatible lymphocytes leads to rapid functional deletion of cytotoxic T lymphocyte precursors. J. Exp. Med. *170*, 679–690.

Mendelson, J., Arkin, S., and Lipton, J.M. (1995). CD102 (ICAM-2) and CD50 (ICAM-3), unlike CD54 (ICAM-1) are constitutively expressed on hematopoietic progenitors. Blood *86, Suppl 1*, 674a.

Nguyen, C., Rocha, D., Granjeaud, S., Baldit, M., Bernard, K., Naquet, P., and Jordan, B.R. (1995). Differential gene expression in the murine thymus assayed by quantitative hybridization of arrayed cDNA. Genomics *29*, 207–216.

Resnick, M.B., and Weller, P.F. (1993). Mechanisms of eosinophil recruitment. Am. J. Resp. Cell. Mol. Biol. *8*, 349–355.

Röhnelt, R.K., Hoch, G., Reiss, Y., and Engelhardt, B. (1997). Immunosurveillance modelled in vitro: naive and memory T cells spontaneously migrate across unstimulated microvascular endothelium. Int. Immunol. *9*, 435–450.

Schmits, R., Filmus, J., Gerwin, N., Senaldi, G., Kiefer, F., Kundig, T., Wakeham, A., Shahinian, A., Catzavelos, C., Rak, J., et al. (1997). CD44 regulates hematopoietic progenitor distribution, granuloma formation, and tumorigenicity. Blood *90*, 2217–2233.

Soriano, S.G., Lipton, S.A., Wang, Y.F., Xiao, M., Springer, T.A., Gutierrez-Ramos, J.C., and Hickey, P.R. (1996). Intercellular adhesion molecule-1 deficient mice are less susceptible to cerebral ischemia-reperfusion injury. Ann. Neurol. *39*, 618–624.

Springer, T.A. (1990). Adhesion receptors of the immune system. Nature *346*, 425–434.

Springer, T.A. (1994). Traffic signals for lymphocyte recirculation and leukocyte emigration: the multistep paradigm. Cell *76*, 301–314.

Tsuyuki, S., Tsuyuki, J., Einsle, K., Kopf, M., and Coyle, A.J. (1997). Costimulation through B7–2 (CD86) is required for the induction of a lung mucosal T helper cell 2 (TH2) immune response and altered airway responsiveness. J. Exp. Med. *185*, 1671–1679.

Wang, B., Biron, C.A., She, J., Higgins, K., Sunshine, M.-J., Lacy, L., Lonberg, N., and Terhorst, C. (1994). A block in both early T lymphocyte and natural killer cell development in transgenic mice with high copy numbers of the CD3-ϵ gene. Proc. Natl. Acad. Sci. USA *91*, 9402–9406.

Xu, H., Tong, I.L., de Fougerolles, A.R., and Springer, T.A. (1992). Isolation, characterization, and expression of mouse ICAM-2 complementary and genomic DNA. J. Immunol. *149*, 2650–2655.

Xu, H., Gonzalo, J.A., St. Pierre, Y., Williams, I.R., Kupper, T.S., Cotran, R.S., Springer, T.A., and Gutierrez-Ramos, J.-C. (1994). Leukocytosis and resistance to septic shock in intercellular adhesion molecule 1-deficient mice. J. Exp. Med. *180*, 95–109.

Xu, H., Bickford, J.K., Luther, E., Carpenito, C., Takei, F., and Springer, T.A. (1996). Characterization of murine intercellular adhesion molecule-2. J. Immunol. *156*, 4909–4914.